Oncogene (2012) 31, 4460–4471

www.nature.com/onc

ORIGINAL ARTICLE

Androgen-regulated miR-32 targets BTG2 and is overexpressed in castration-resistant prostate cancer

SE Jalava[1], A Urbanucci[1], L Latonen[1], KK Waltering[1], B Sahu[2], OA Jänne[2], J Seppälä[3], H Lähdesmäki[4], TLJ Tammela[5] and T Visakorpi[1]

[1]*Institute of Biomedical Technology, Tampere University, Tampere, Finland;* [2]*University of Helsinki, Institute of Biomedicine Physiology, Biomedicum Helsinki, Helsinki, Finland;* [3]*Department of Signal Processing, Tampere University of Technology, Tampere, Finland;* [4]*Department of Information and Computer Science, Aalto University School of Science, Helsinki, Finland and* [5]*Department of Urology, University of Tampere and Tampere University Hospital, Tampere, Finland*

The androgen receptor (AR) signaling pathway is involved in the emergence of castration-resistant prostate cancer (CRPC). Here, we identified several androgen-regulated microRNAs (miRNAs) that may contribute to the development of CRPC. Seven miRNAs, miR-21, miR-32, miR-99a, miR-99b, miR-148a, miR-221 and miR-590-5p, were found to be differentially expressed in CRPC compared with benign prostate hyperplasia (BPH) according to microarray analyses. Significant growth advantage for LNCaP cells transfected with pre-miR-32 and pre-miR-148a was found. miR-32 was demonstrated to reduce apoptosis, whereas miR-148a enhanced proliferation. Androgen regulation of miR-32 and miR-148a was confirmed by androgen stimulation of the LNCaP cells followed by expression analyses. The AR-binding sites in proximity of these miRNAs were demonstrated with chromatin immunoprecipitation (ChIP). To identify target genes for the miRNAs, mRNA microarray analyses were performed with LNCaP cells transfected with pre-miR-32 and pre-miR-148a. Expression of *BTG2* and *PIK3IP1* was reduced in the cells transfected with pre-miR-32 and pre-miR-148a, respectively. Also, the protein expression was reduced according to western blot analysis. *BTG2* and *PIK3IP1* were confirmed to be targets by 3′UTR-luciferase assays. Finally, immunostainings showed a statistically significant ($P<0.0001$) reduction of BTG2 protein in CRPCs compared with untreated prostate cancer (PC). The lack of BTG2 staining was also associated ($P<0.01$) with a short progression-free time in patients who underwent prostatectomy. In conclusion, androgen-regulated miR-32 is overexpressed in CRPC, leading to reduced expression of BTG2. Thus, miR-32 is a potential marker for aggressive disease and is a putative drug target in PC.
Oncogene (2012) **31,** 4460–4471; doi:10.1038/onc.2011.624; published online 23 January 2012

Keywords: neoplasia; prostatic; miR-32; BTG2; hormone refractory; androgen independent

Correspondence: Professor T Visakorpi, Institute of Biomedical Technology, Tampere University, Tampere FIN-33014, Finland.
E-mail: tapio.visakorpi@uta.fi
Received 24 February 2011; revised 4 November 2011; accepted 2 December 2011; published online 23 January 2012

Introduction

The androgen receptor (AR) signaling pathway is crucial in the development and progression of prostate cancer (PC). Androgen deprivation therapy has been the standard treatment for advanced tumors for over half a century. Initially, almost all tumors respond to the therapy; however, the disease eventually progresses, and castration-resistant prostate cancer (CRPC) emerges. For CRPC, there is no curative treatment available (Massard and Fizazi, 2011). Despite the low levels of androgens during castration, the AR signaling pathway seems to still be active (Chen *et al*., 2004; Attard *et al*., 2008). The AR is overexpressed in CRPC, which is partially explained by gene amplification (Visakorpi *et al*., 1995; Linja *et al*., 2001; Edwards *et al*., 2003). Also, other mechanisms for the activation of AR signaling have been suggested, including AR mutations, ligand-independent activation and changes in coregulatory molecules (Scher and Sawyers, 2005).

Several AR-regulated genes, such as *KLK3* (prostate-specific antigen (PSA)) and the *TMPRSS2:ERG* fusion transcript, are reactivated in CRPC (Feldman and Feldman, 2001; Stanbrough *et al*., 2006; Cai *et al*., 2009). However, the target genes that drive the formation of CRPC are not known. For example, the *TMPRSS2:ERG* fusion is found at comparable frequencies in PC and CRPC, suggesting that there is no selective pressure for the fusion during the emergence of CRPC (Saramäki *et al*., 2008; Tomlins *et al*., 2009; Leinonen *et al*., 2010).

MicroRNAs (miRNAs) are a class of small, non-coding RNAs that can regulate up to 60% of protein-coding genes by binding to the 3′ untranslated region (UTR) sequences of target mRNAs (Bartel, 2009; Friedman *et al*., 2009). miRNAs are highly tissue specific. A single miRNA can have several different target genes and thus can target different mRNAs in different cellular environments (Kloosterman and Plasterk, 2006). Since the discovery of miRNAs, there has been growing evidence of miRNA dysregulation in different cancers. It has been shown that miRNAs can function as oncogenes and tumor-suppressor genes (Di Leva and Croce, 2010).

A few miRNA expression profiling studies have previously been done on PC (Lu *et al*., 2005; Volinia *et al*., 2006; Schaefer *et al*., 2010; Martens-Uzunova *et al*., 2011). However, only a few CRPC samples have been included in these studies (Porkka *et al*., 2007). Here, miRNA expression profiling was performed on a clinical tumor sample set consisting of untreated and castration-resistant tumors and benign controls to identify differentially expressed miRNAs. Expression data were integrated with data of AR-binding sites (ARBSs) in LNCaP cells, detected by chromatin immunoprecipitation and sequencing (ChIP-seq). Using this approach we identified miRNAs that were both differentially expressed in CRPC and potentially regulated by androgen. We showed that miR-32 and miR-148a are regulated by androgen and are overexpressed in CRPC. Functional studies showed that miR-32 reduces apoptosis and that miR-148a enhances proliferation in PC cells. We also identified putative target genes for miR-32 and miR-148a: *BTG2* (*B-cell translocation gene 2*) and *PIK3IP1* (*phosphoinositide-3-kinase interacting protein 1*), respectively. Finally, we demonstrated a loss of BTG2 expression in CRPC and its association with prognosis in hormone-naive PC.

Results

Androgen receptor-binding sites

We profiled ARBSs on chromatin of cell line model, which we have previously established by stable transfection of AR to LNCaP cells (Waltering *et al*., 2009). The model contains three sublines of LNCaP; the empty vector transfected control cells, LNCaP-pcDNA3.1, as well as LNCaP-ARmo and LNCaP-ARhi, expressing 2–3-fold and 4–5-fold more AR than the control cells, respectively. Using ChIP-seq, we obtained ARBS maps of all the LNCaP sublines upon stimulation with 1 and 100 nM 5α-dihydrotestosterone (DHT) as compared with nonstimulated cells (0 M). We identified with ChIP-seq altogether 414 miRNAs with proximal ARBSs (Supplementary Table S1). In LNCaP-pcDNA3.1 treated with 100 nM DHT, we found 197 miRNAs with ARBS. In LNCaP-ARmo and in LNCaP-ARhi cells the number of miRNAs with binding sites were 172 and 161 in 1 nM DHT-treated sample, respectively (Table 1). ARBSs were searched upstream of miRNA start site, or transcription start site of the host gene in case of intragenic miRNA. If ARBS that was found was nearest to the miRNA compared with any other gene, ARBS was thought to belong to the miRNA. All the miRNAs showing ARBSs in at least one of the samples are listed in Supplementary Table S1.

miRNA expression profiling of clinical samples

miRNA expression profiling was conducted using clinical samples of 5 benign prostatic hyperplasia (BPH) and 28 PCs obtained from prostatectomies or cystoprostatectomies, as well as 7 BPH and 14 CRPCs obtained from transurethral resections of the prostate (TURPs). Because of different expression patterns obtained from prostatectomy and TURP specimens, these two classes were kept separate in the analysis (Supplementary Figure S1). A total of 411 (57%) out of 723 human miRNAs included in the array were considered significantly expressed.

Table 1 Number of miRNAs that show ARBS in different samples and DHT concentrations

Sample and DHT conc.	*Number of miRNAs with ARBS*
pcDNA3.1_0 nm	105
pcDNA3.1_1 nm	109
pcDNA3.1_100 nm	197
ARmo_0 nm	63
ARmo_1 nm	172
ARmo_100 nm	104
ARhi_0 nm	36
ARhi_1 nm	161
ARhi_100 nm	93

Abbreviations: ARBS, androgen receptor-binding site; ARhi, LNCaP AR high expression; ARmo, LNCaP AR moderate expression; conc., concentration; DHT, 5α-dihydrotestosterone; miRNA, microRNA; pcDNA3.1, LNCaP pcDNA3.1-transfected control.

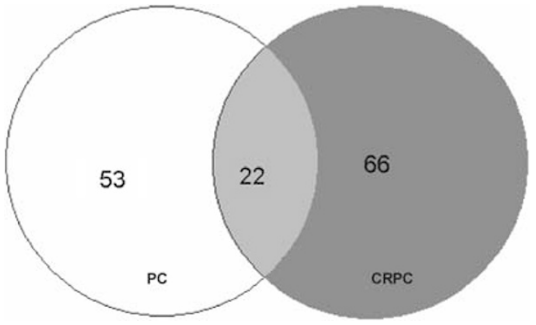

Figure 1 Venn diagram of differentially expressed genes in PC and CRPC according to the miRNA microarray.

miRNAs were considered to be differentially expressed in PC compared with BPH if >1.5-fold change and a *P*-value of <0.05 according to Welch's *t*-test were observed. According to these criteria, 75 miRNAs were differentially expressed in PC, and 88 were differentially expressed in CRPC (Supplementary Tables S2 and S3). Of these, 22 miRNAs were found to be differentially expressed in both PC and CRPC compared with their controls (Figure 1).

The androgen regulation of the miRNAs that had interesting expression pattern according to the microarray were evaluated by utilizing the expression data from our previous study (Waltering *et al*., 2010) and the ARBSs in the LNCaP-derived sublines. Finally, seven miRNAs were selected for functional studies. Five of the miRNAs were regulated by DHT and showed putative ARBSs upstream without other genes nearby, namely, miR-32, miR-148a, miR-99a, miR-21 and miR-221. Two more miRNAs, miR-590-5p and miR-99b were also

Table 2 Mean expression values of putative androgen-regulated miRNAs in clinical samples according to the microarray

Systematic name of the miRNA	*Corrected* P-*value*	*Fold change*	*Regulation*	*BPH*	*PC*	*BPH TURP*	*CRPC*
hsa-miR-32	0.00126	5.8	Up	3.92	4.30	0.49	3.03
hsa-miR-590-5p	0.00356	2.8	Up	5.37	4.93	3.50	4.99
hsa-miR-148a	0.04345	2.9	Up	10.47	11.04	8.45	9.98
hsa-miR-21	0.00694	2.1	Up	13.15	13.30	12.00	13.06
hsa-miR-99a	0.04490	2.3	Down	11.45	11.12	11.08	9.85
hsa-miR-99b	0.00126	2.8	Down	7.24	7.26	8.20	6.70
hsa-miR-221	0.00280	4.6	Down	10.02	8.55	8.97	6.76

Abbreviations: BPH, benign prostatic hyperplasia; BPH TURP, BPH obtained from transurethral resection of the prostate; CRPC, castration-resistant prostate cancer; miRNA, microRNA; PC, primary untreated prostate cancer.

regulated by DHT and they had ARBSs in close proximity of miRNA but however closer to other genes. Four of these, namely miR-32, miR-590-5p, miR-148a and miR-21, were significantly overexpressed, and three, miR-99a, miR-99b and miR-221, were significantly underexpressed in CRPC (Table 2 and Supplementary Figure S2). All of them, except miR-221, were found to be differentially expressed only in CRPC and not in PC. Because both miR-21 and miR-221 have previously shown to be androgen regulated and implicated in CRPC, they were omitted from further studies (Ribas *et al*., 2009; Sun *et al*., 2009).

Functional evaluation of miRNAs

Precursor miRNA (pre-miR) oligonucleotides for miR-32, miR-590-5p, miR-148a, miR-99b and miRNA inhibitor construct (anti-miR) for miR-99a were transfected into parental LNCaP cells to determine their effects on cell growth. Two of the miRNAs, miR-32 and miR-148a, significantly enhanced the growth rate ($P<0.05$ at day 5) of LNCaP cells (Figure 2a), whereas the other miRNAs showed no significant effect (Supplementary Figure S3). The transfection of these two pre-miRNAs increases the levels of miR-32 and miR-148a in LNCaP cells (Figure 2b).

The effects of miR-32 and miR-148a were further studied in the presence and absence of androgens. As shown in Figures 2c and d, both miR-32- and miR-148a-transfected LNCaP cells grew better than control transfected in 15 nM DHT. However, the effect of miR-32 transfection was abolished in hormone-starved conditions (Figure 2c), whereas the forced expression of miR-148a maintained the growth advantage over control cells even upon hormone starvation (Figure 2d). Cell cycle analysis showed that apoptosis was significantly reduced in miR-32-transfected LNCaP cells compared with scrambled-oligo-transfected cells, indicating increased cell survival. The number of cells in S or G2 phase did not change (Figure 2e). Cleaved-caspase-3 staining showed significantly less stained cells in miR-32-transfected compared with control-transfected cells 3 days after transfection (Figure 2f). In the case of miR-148a, cell cycle analysis showed that miR-148a expression significantly increased the number of cells in the S phase (Figure 2e).

Androgen regulation of miR-32 and miR-148a

We have previously shown that the expression of miR-32 and miR-148a is stimulated by DHT treatment of LNCaP cells based on our AR overexpression model (LNCaP-ARmo and LNCaP-ARhi) (Waltering *et al*., 2010) To confirm this finding, parental LNCaP cells were stimulated with 0, 1 and 10 nM DHT for 6 h, and the expression of miR-32 and miR-148a was analyzed by quantitative real-time PCR (qRT–PCR). Upregulation of miR-32 and miR-148a was clearly observed upon DHT stimulation (Figure 3a).

miR-32 is located on chromosome 9 in the intron 14 of c9orf5. According to the ARBS map produced in the LNCaP AR-overexpressing model, an ARBS in located in the tenth intron of the c9orf5 gene, approximately 14 kb upstream of the miR-32 locus (Figure 3b). The ARBS was confirmed by ChIP-qPCR (Figure 3c). After 2 h of stimulation with 1 nM DHT, both LNCaP-pcDNA3.1 and LNCaP-ARhi cells showed AR increased binding compared with IgG and ethanol (nonstimulated) controls.

miR-148a is located on chromosome 7. According to our ARBS map, there are two ARBSs in close proximity to miR-148a, one 72 kb upstream and the other 8.5 kb downstream (Figure 3d). Both of these ARBSs were confirmed by ChIP–qPCR (Figures 3e and f). Interestingly, all the confirmed ARBSs showed increased AR binding in AR-overexpressing compared with control cells (LNCaP-pcDNA3.1).

Identification of target genes for miR-32 and miR-148a

To identify target genes for miR-32 and miR-148a, mRNA microarray analysis was performed with LNCaP cells transfected with pre-miR-32 and pre-miR-148a (Supplementary Tables S4 and S5). Among the twofold downregulated genes after pre-miR-32 transfections, there were six genes that three different target prediction programs, Pictar (http://pictar.mdc-berlin.de/), Target Scan (www.targetscan.org) and miRanda (www.microrna.org), predicted to be the targets for miR-32. These were *MYO1B, FBN1*, *BTG2*, *MAN2A1*, *RNF38* and *SNN*. Of these, *BTG2* was functionally most promising and it was selected for further validation. Downregulation of *BTG2* in LNCaP cells transfected with pre-miR-32 was confirmed by qRT–PCR (Figure 4a) and western blot (Figure 4b). None of the 50 most downregulated

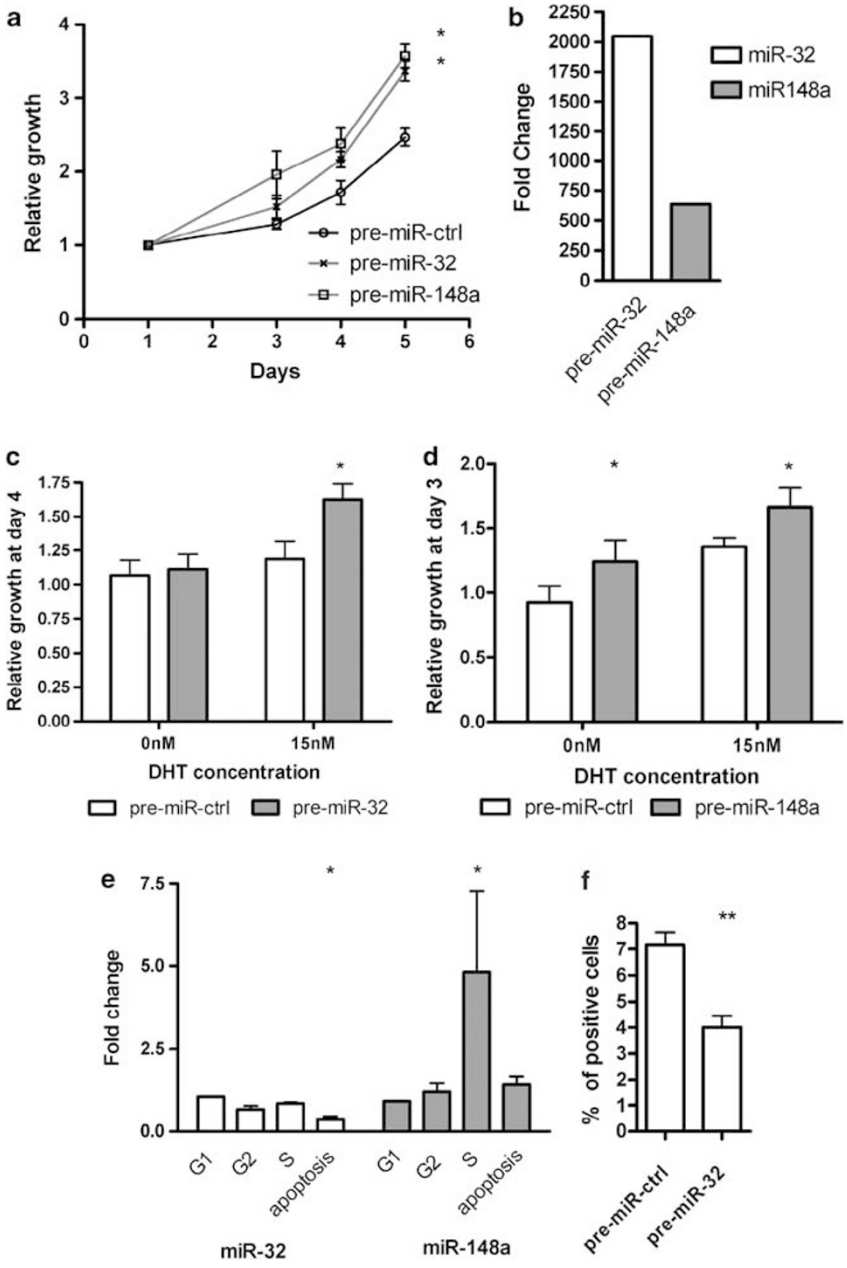

Figure 2 (**a**) Growth curves of LNCaP cells transfected with pre-miR-control, pre-miR-32 or pre-miR-148a. The mean cell number ± s.d. on different days is shown. Statistical significance was assessed by Mann–Whitney *U*-tests. (**b**) Forced expression of miR-32 and miR-148a by pre-miRNA transfections. qRT–PCR analysis was performed 3 days after transfection, and levels of miR-32 and miR-148a are reported. (**c**) Relative growth of DHT-treated (0 or 15 nM) LNCaP cells transfected with pre-miR-32 at day 4 after transfection. The means ± s.e.m. are shown. Statistical significance was assessed by Mann–Whitney *U*-test. (**d**) Relative growth of DHT-treated (0 or 15 nM) LNCaP cells transfected with pre-miR-148a at day 3 after transfection. The means ± s.e.m. are shown. Statistical significance was assessed by Mann–Whitney *U*-test. (**e**) Results of PI staining and cell cycle analysis by flow cytometry of LNCaP cells after pre-miR-control, pre-miR-32 or pre-miR-148a transfections. The means ± s.d. are shown, and significance was assessed by Welch's *t*-test. (**f**) Proportion of caspase-3-positive LNCaP cells 3 days after pre-miR-control or pre-miR-32 transfection. The means ± s.d. are shown, and significance was assessed by Welch's *t*-test.

genes in pre-miR-148a-transfected LNCaP cells were predicted target genes for miR-148a by target prediction programs Pictar, TargetScan and miRanda. However, *PIK3IP1*, which was among the 20 most downregulated genes, was selected for further studies (Supplementary Table S5). *PIK3IP1* was selected based on the function of the protein, as phosphatidylinositol-3-kinase (PI3K) signaling is considered to be one of the most commonly altered pathways in PCs (Taylor *et al*., 2010). Downregulation of *PIK3IP1* in LNCaP cells transfected with pre-miR-148a was confirmed by qRT–PCR (Figure 4c) and western blot (Figure 4d).

To show the direct interaction between miRNAs and putative targets, we performed luciferase reporter

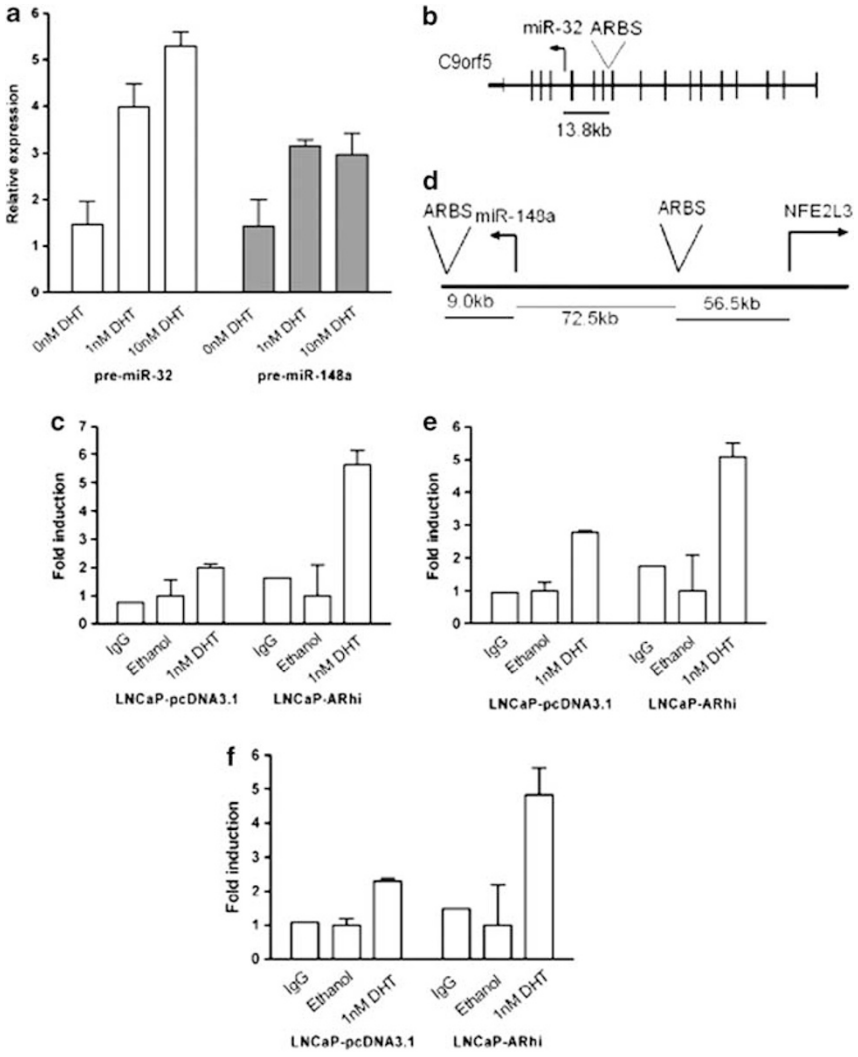

Figure 3 (**a**) The expression (mean ± s.d.) of miR-32 (white bars) and miR-148a (gray bars) at 6 h post stimulation with 0, 1 or 10 nM DHT according to qRT–PCR. Experiments were performed in triplicate, and values are normalized to RNU44. (**b**) Schematic illustration of an identified ARBS in the intron of C9orf5 near the miR-32 genomic location. Black lines illustrate exons in the C9orf5 gene. (**c**) Confirmation of AR binding to the ARBS near the miR-32 genomic location shown in (**b**). qPCR analysis of ChIP samples after DHT (1 nM) stimulation of LNCaP-pcDNA3.1 and LNCaP-ARhi cells. Ethanol-stimulated and IgG-immunoprecipitated cells were used as controls. The means ± s.d. are shown. (**d**) Schematic illustration of identified ARBSs near the miR-148a genomic location. (**e**, **f**) Confirmation of ARBS near the miR-148a (upstream and downstream) genomic location shown in (**d**). qPCR of ChIP samples after DHT (1 nM) stimulation of LNCaP-pcDNA3.1 and LNCaP-ARhi cells. Ethanol-stimulated and IgG-immunoprecipitated cells were used as controls. The means ± s.d. are shown.

assays. Luciferase plasmids containing either the *BTG2* 3′UTR or the *PIK3IP1* 3′UTR were transfected together with pre-miR-control, pre-miR-32 or pre-miR-148a into LNCaP cells. Inhibition of luciferase activity was observed when the *BTG2* 3′UTR was transfected together with miR-32, but not with miR-control or miR-148a. Similarly, inhibition of luciferase activity was observed when the PIK3IP1 3′UTR was transfected with miR-148a, but not with the control miRNAs (Figure 4e). BIM has previously been suggested to be a target of miR-32 in LNCaP cells (Ambs *et al*., 2008). However, *BIM* was not downregulated in our mRNA microarray study in cells overexpressing miR-32 (Supplementary Table S4). Additionally, the level of BIM protein was not reduced in miR-32-transfected cells according to the western blot analysis (Supplementary Figure S4). Recently, miR-148a was shown to target CAND1 in PC cells (Murata *et al*., 2010). However, *CAND1* mRNA was not reduced in the pre-miR-148a-transfected LNCaP cells (Supplementary Table S5).

To confirm whether BTG2 downregulation by miR-32 is responsible for growth advantage of the miR-32-transfected LNCaP cells, a rescue experiment was performed. For this, we used a BTG2 coding sequence (BTG2-CDS) construct lacking the 3′UTR with the potential miR-32-binding sites. LNCaP cells were co-transfected with pSG5 plasmid with and without BTG2-CDS together with pre-miR-32 or pre-miR-ctrl. BTG2-CDS reduced growth of the miR-32-transfected LNCaP by day 5, whereas LNCaPs co-transfected with

miR-32 and empty vector continued to grow (Supplementary Figure S5).

BTG2 and PIK3IP1 expression in clinical samples

Tissue microarrays containing both prostatectomy specimens ($n=170$) and CRPC-TUPR ($n=94$) specimens were stained using antibodies against BTG2 and PIK3IP1. The BTG2 antibody resulted in a strong, predominantly cytoplasmic staining in the nonmalignant luminal epithelia, whereas the PIK3IP1 antibody showed strong staining in both the nucleus and cytoplasm of luminal epithelial cells (Figures 5a–d). The basal cells showed strong nuclear staining with the PIK3IP1 antibody. The staining intensity was generally decreased in malignant cells. CRPC cells showed significantly ($P<0.0001$) lower staining intensities compared with PC with the BTG2 antibody, whereas no differences were observed with the PIK3IP1 antibody (Figures 5e and f). In prostatectomy specimens, low BTG2 staining was associated with a higher pT stage (pT3 vs pT2, $P=0.009$, χ^2 test), but not with Gleason score ($P=0.0868$, χ^2 test) or diagnostic PSA value ($P=0.2789$, analysis of variance (ANOVA)). The absence of BTG2 expression was also significantly associated with a short, cancer progression-free period ($P=0.0021$, Mantel–Cox test) (Figure 5g). Low PIK3IP1 staining was associated with higher diagnostic PSA values ($P=0.0404$, ANOVA; according to Bonferroni's test, the significant difference was between staining intensity 3 vs 0), but not with pT stage ($P=0.7190$, χ^2 test), Gleason score ($P=0.2007$, χ^2 test) or progression-free survival ($P=0.3676$, Mantel–Cox test).

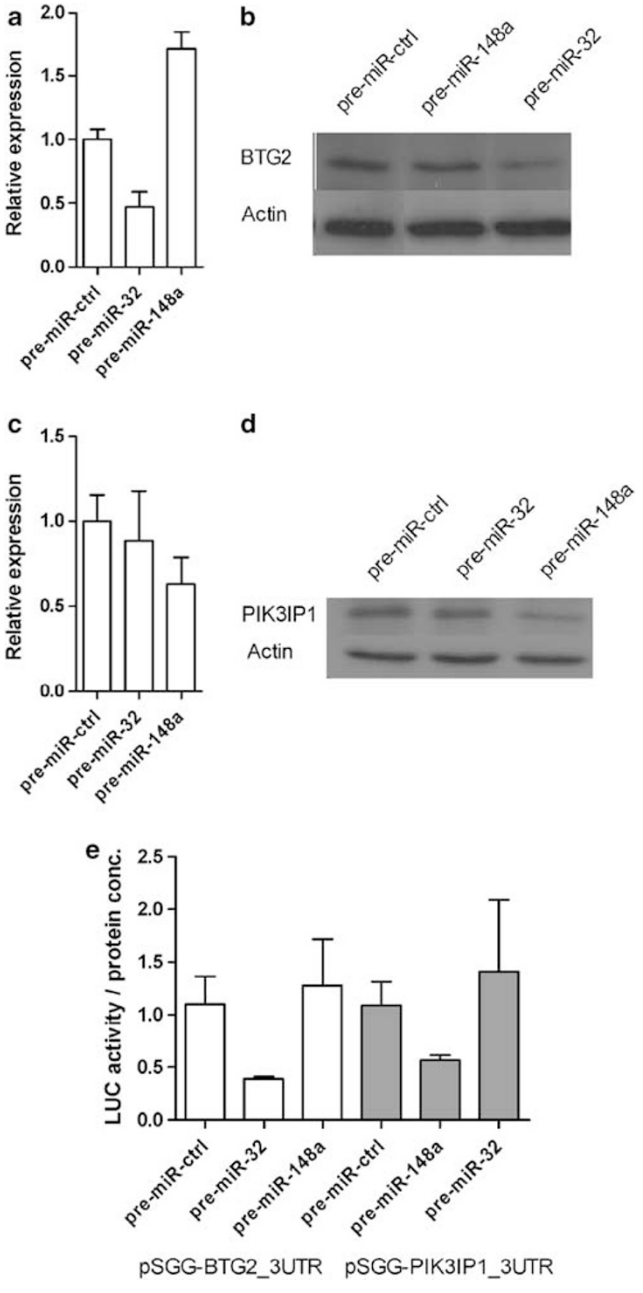

Figure 4 (**a**) Inhibition of *BTG2* mRNA expression by miR-32. qRT–PCR analysis of *BTG2* levels in LNCaP cells transfected with pre-miR-control, pre-miR-148a or pre-miR-32. RNA was extracted 3 days after transfection. Values are normalized to *TBP*. (**b**) Inhibition of BTG2 protein expression by miR-32. Protein was extracted from LNCaP cells transfected with pre-miR-control, pre-miR-148a or pre-miR-32 at 4 days after transfection. Loading: 15 μg of cytoplasmic protein fraction. (**c**) Inhibition of *PIK3IP1* mRNA expression by miR-148a. qRT–PCR analysis of *PIK3IP1* levels in LNCaP cells transfected with pre-miR-control, pre-miR-32 or pre-miR-148a. RNA was extracted 3 days after transfection. Values are normalized to *TBP*. (**d**) Inhibition of PIK3IP1 protein expression by miR-32. Protein was extracted from LNCaP cells transfected with pre-miR-control, pre-miR-32 or pre-miR-148a at 4 days after transfection. Loading: 15 μg of total protein. (**e**) miR-32 and miR-148a inhibit the expression of *BTG2* and *PIK3IP1*, respectively, by 3′UTR-mediated mechanisms. Luciferase assays were performed on LNCaP cells co-transfected with pSGG carrying the *BTG2* 3′UTR region (white bars) or the *PIK3IP1* 3′UTR region (gray bars) and pre-miR-control, pre-miR-32 or pre-miR-148a. Values are normalized to total protein concentrations. The means ± s.d. are shown.

Discussion

We utilized miRNA expression profiling of CRPC to identify miRNAs that are important in the onset of CRPC. By combining expression data of clinical samples with androgen-regulated miRNAs and ARBSs, we found seven miRNAs that are both differentially expressed in CRPC and putatively regulated by androgen. Functional studies of these miRNAs indicated that miR-32 and miR-148a could be important in the emergence of CRPC.

In miRNA expression arrays of clinical samples, upregulation of miR-32 and miR-148a was found in CRPC but not in PC. However, in a subset of PC samples, moderate upregulation of miR-32 was observed. In addition, increased expression of miR-32 has previously been reported in localized PC (Ambs *et al*., 2008). We have also previously identified an expression

panel of miRNAs that predict poor outcome after prostatectomy (Martens-Uzunova *et al*., 2011). miR-32 was one of the miRNAs in the panel. Thus, it is possible that the overexpression of these miRNAs does not occur exclusively in CRPC but may occur earlier in PC progression. However, we observed especially strong overexpression of miR-32 in CRPC. In contrast to our data, the expression of miR-148a has been suggested to be reduced in CRPC cell lines (Fujita *et al*., 2010). Thus, it is critical to study the expression of miRNAs in not only cancer cell lines, but also clinical samples. Similarly, some studies have shown high expression of miR-221 in castration-resistant cell line phenotype (Sun *et al*., 2009). However, we and others have shown in clinical samples that the expression of miR-221 is downregulated in PC and CRPC (Schaefer *et al*., 2010; Spahn *et al*., 2010). There are several cases in which the expression in cell lines does not correspond to the expression in tissue specimens. This may be because of the fact that in cell lines, mRNAs often have shortened 3′UTRs, and target genes for miRNAs might be different *in vitro* than *in vivo* (Sandberg *et al*., 2008).

The functional significance of miR-32 and miR-148a in PC cells was studied by transfecting pre-miRNAs into the androgen-sensitive PC cell line LNCaP. Their transfections enhanced cell growth. In the case of miR-32, growth enhancement was abolished when cells were cultured in low levels of androgens, whereas miR-148a enhanced the growth of LNCaP cells in the absence of androgens. Further studies revealed that this enhancement was because of the reduction of apoptosis in pre-miR-32 and increase of cell proliferation in pre-miR-148a-transfected cells. However, it should be noted that pre-miR transfections increase dramatically the levels of the transfected miRNA that does not mimic the biological levels of miRNA expression. However, pre-miR transfection is an established way of studying miRNA functions in cell lines.

We demonstrated that there was a significant upregulation of miR-32 and miR-148a in LNCaP cells grown in the presence of 1 nM DHT. We were also able to confirm the presence of ARBSs in close proximity to both of the miRNA genomic loci by ChIP–qPCR. The same ARBSs are also shown by ChIP-seq analysis of two xenografted tumors originating from CRPC patients (Urbanucci *et al*., 2011). This finding confirms that such ARBSs are not only LNCaP specific but can also be found *in vivo*. The androgen responsiveness of miR-148a expression was suggested by Murata *et al*. (2010), confirming our data. We identified two different ARBSs for miR-148a, one locating downstream and one upstream from the miRNA genomic location. Upstream ARBS has *NFE2L3* gene in relatively close (130 kb);

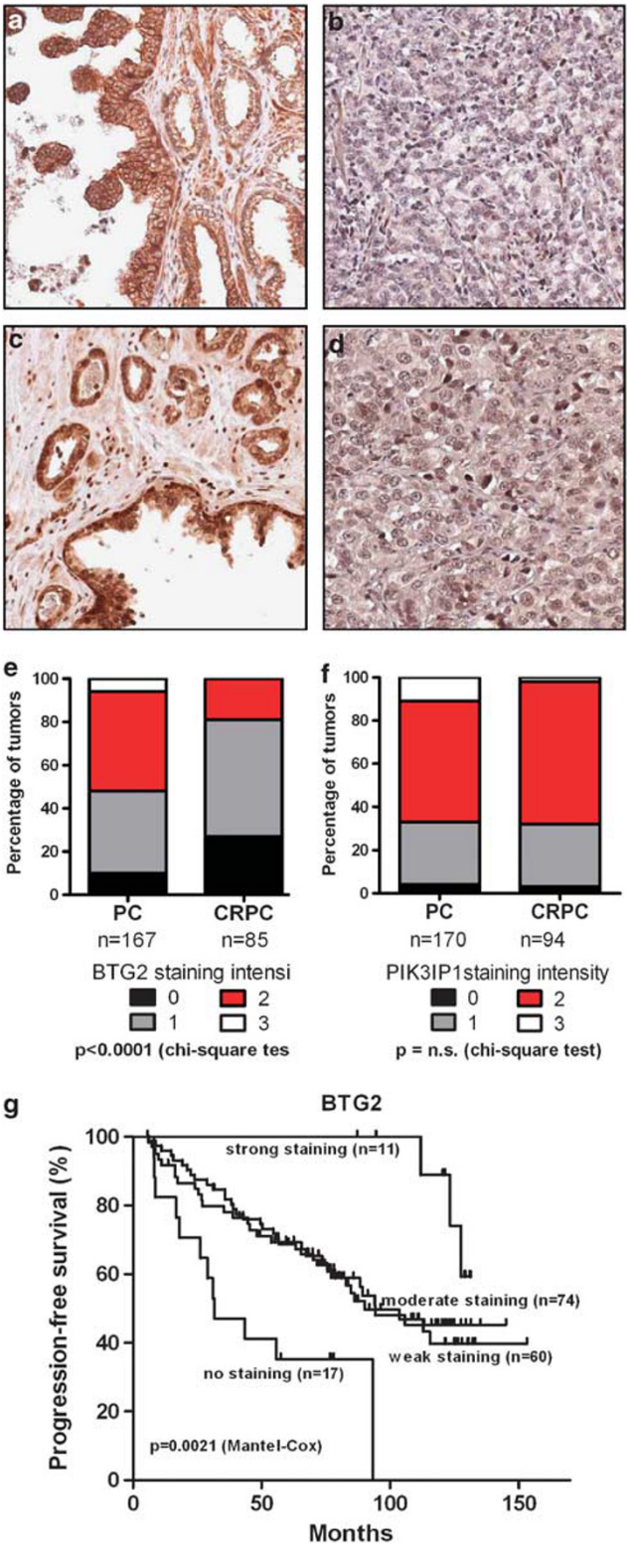

Figure 5 Immunostaining of PC (**a**, **c**) and CRPC (**b**, **d**) PCs with anti-BTG2 (**a**, **b**) and anti-PIK3IP1 (**c**, **d**) antibodies. The nonmalignant epithelia (**a**, **c**) show strong staining with both antibodies, but the malignant cells show reduced staining with the anti-BTG2 antibody. The CRPCs show a lack of staining with anti-BTG2 (**b**) and very weak staining with anti-PIK3IP1 (**d**). Scoring of the staining intensities with anti-BTG2 (**e**) and anti-PIK3IP1 (**f**) indicates that BTG2 protein expression is significantly reduced in CRPC compared with PC, whereas no association is found with PIK3IP1 expression. (**g**) Kaplan–Meier curves of progression-free survival of the prostatectomy-treated patients according to BTG2 staining.

however this ARBS is closer to miR-148a (72 kb). Still, further evaluations are needed in order to clarify whether this upstream ARBS regulates miR-148a transcription.

Identification of miRNA targets is challenging. Recently, it was shown that predominant miRNA action decreases target mRNA levels, making expression arrays an efficient tool to identify novel miRNA targets (Guo *et al*., 2010). Using mRNA expression arrays of LNCaP cells transfected with pre-miRNAs, we were able to identify putative target genes for both miR-32 and miR-148a. For miR-32, we identified the novel putative target gene *BTG2*. BTG2 was downregulated at both the mRNA and protein levels in LNCaP cells transfected with pre-miR-32. In addition, luciferase reporter assays confirmed that miR-32 targets the 3′UTR of *BTG2*. We also performed a rescue experiment co-transfecting miR-32 with and without BTG2 to LNCaP cells. Growth reduction of BTG2-expressing LNCaP cells was seen 5 days after co-transfections, whereas cells transfected with miR-32 and empty vector control still continued growing. This suggests that indeed BTG2 downregulation is the main reason for growth advantage seen in miR-32-transfected LNCaP cells. By immunohistochemistry, we showed that the protein expression of BTG2 is reduced in PC. Notably, BTG2 expression was almost completely abolished in the majority of CRPC specimens, whereas miR-32 expression was highly upregulated. This finding further confirms that BTG2 is a target of miR-32; however, we cannot rule out other mechanisms for BTG2 downregulation. The loss of BTG2 expression was also significantly associated with a short, cancer progression-free period in prostatectomy-treated patients, suggesting that BTG2 is a putative biomarker of PC aggressiveness.

BTG2 expression has previously been reported to be lost or reduced in several cancers, including breast and PCs (Ficazzola *et al*., 2001; Möllerström *et al*., 2010). In PC, BTG2 downregulation has been suggested to be an early event (Ficazzola *et al*., 2001). Although the most striking finding was the loss of expression in CRPC, we also found reduced expression of BTG2 in a subset of PC specimens. BTG2 seems to be involved in several cellular processes, including cell cycle control and apoptosis (Hong *et al*., 2005; Winkler, 2010). BTG2 belongs to a BTG/Tob family of six proteins and has been demonstrated to have antiproliferative activities (Winkler, 2010). Forced expression of BTG2 in another PC cell line, PC-3, has been shown to decrease cell proliferation and tumorigenicity *in vivo* (Ficazzola *et al*., 2001). We observed decreased apoptosis in miR-32-transfected LNCaP cells, which could occur through the pro-apoptotic functions of BTG2. Interestingly, it has recently been suggested that BTG2 could be a corepressor of AR (Hu *et al*., 2011). Thus, miR-32/BTG2 could form a positive feedback loop of AR signaling in PC.

PIK3IP1 was identified as a putative target gene for miR-148a. PIK3IP1 was downregulated at mRNA and protein levels after transfection of LNCaP cells with pre-miR-148a. In addition, miR-148a binding to the 3′UTR region of *PIK3IP1* was confirmed by luciferase reporter assays. Of note, the target prediction programs did not identify PIK3IP1 as a potential target for miR-148a. By immunostaining, we found that the expression of PIK3IP1 is reduced in PC, although the reduction was not as clear as for BTG2. PIK3IP1 is a relatively recently identified PI3K regulating protein. PIK3IP1 binds directly to PI3K and negatively regulates its activity (Zhu *et al*., 2007). PI3K pathway activation is seen in many types of cancers, and the pathway regulates several cellular processes that are critical for cancer progression, including metabolism, growth and survival (Courtney *et al*., 2010). Furthermore, PI3K signaling is considered to be one of the most commonly altered pathways in both primary and metastatic PCs (Taylor *et al*., 2010). Our data link the PI3K and AR pathways, which are both important to PC progression.

Finally, the data here confirm our previous findings (Urbanucci *et al*., 2011) indicating that chromatin binding of AR takes place in lower DHT concentrations in the cells overexpressing the receptor. Thus, the overexpression seems to make cancer cells hypersensitive to the low levels of residual androgens in patients even after castration.

In conclusion, we identified two androgen-regulated miRNAs, miR-32 and miR-148a, that are upregulated in CRPC. Androgen regulation was observed after 6 h of DHT stimulation, and novel ARBSs were identified for both of the miRNAs. We further demonstrated that miR-32 is involved in cell survival, as forced expression of miR-32 protects cancer cells from apoptosis. Furthermore, BTG2 was identified as a miR-32 target, and BTG2 expression was shown to be associated with the aggressiveness of prostate tumors. These findings suggest that miR-32 is an androgen-regulated oncomir in CRPC.

Materials and methods

Cell lines and clinical samples

LNCaP cells were purchased from ATCC (Rockville, MD, USA) and cultured according to the recommended conditions. LNCaP cells transfected with pcDNA3.1 without (LNCaP-pcDNA3.1) or with (LNCaP-ARhi) wild-type AR-cDNA (Waltering *et al*., 2009) were used in the identification of ARBSs.

A total of 54 clinical specimens for microarray analysis were obtained from Tampere University Hospital (TAUH). These include freshly frozen samples of 5 BPH and 28 untreated primary prostate tumors obtained from radical prostatectomy specimens as well as 7 BPH and 14 CRPC tumors obtained from TURP. All specimens were histologically examined and contained $>70\%$ cancerous or hyperplastic tissue. Tissue microarrays of formalin-fixed, paraffin-embedded PC specimens of 170 prostatectomies as well as CRPC specimens of 94 TURPs were constructed from specimens obtained from TAUH. The pT-distribution of prostatectomy cases was pT2: 116, pT3: 52 and pTX: 2. The Gleason score distribution was <7: 69, 7: 81, >7: 18 and X: 2. The mean ($\pm$ s.d.) of diagnostic PSA was 14.1 ± 11.7 ng/ml. According to standard practice, the serum PSA levels of prostatectomy patients were monitored at TAUH for 1 year after the operation and,

subsequently, at least once a year at the local health centers of the Hospital District. Serum PSA values and dates were retrieved from health centers in addition to the patient files at TAUH. The median follow-up time was 71 months (range 6–153). Detectable PSA values ($\geqslant 0.5$ ng/ml) in two consecutive measurements or the emergence of metastases were considered signs of progression. For the CRPCs, the median time from diagnosis (that is, onset of treatment) to TURP (that is, progression) was 34 months (range 3–160 months). The use of clinical material has been approved by Ethical Committee of the TAUH and the National Authority for Medicolegal Affairs.

ChIP-seq and analysis

The description is given in more detail elsewhere (Urbanucci *et al*., 2011). Briefly, cells were hormone deprived for 4 days and treated with DHT at different concentrations for 2 h. Cells were fixed (Merck KGaA, Darmstadt, Germany), pelleted and lysed. The chromatin was immunoprecipitated with 10 μg of normal rabbit IgG (Santa Cruz Inc., Santa Cruz, CA, USA) or 10 μl of AR antibody (Karvonen *et al*., 1997; Thompson *et al*., 2006; Sahu *et al*., 2011; Urbanucci *et al*., 2011). The libraries of ChIP DNA were prepared according to and sequenced with Genome Analyzer II (Illumina Inc., San Diego, CA, USA) according to the manufacturer's protocol. The raw reads alignment was carried out with Bowtie (Langmead *et al*., 2009) and the reads were mapped on the human genome version 19 (hg19). The peak detection was performed with the tool MACS, using default parameters for *P*-value and bandwidth (Zhang *et al*., 2008). ARBS was decided to belong to the miRNA if the ARBS was closest to the miRNA, and not the transcription start site of any other gene. For intragenic miRNAs that are in the same orientation than the host gene, ARBS was search upstream from transcription start site of the host gene. Again, miRNA was given ARBS if the host gene transcription start site was closest to the ARBS. If miRNA is in reverse orientation than host gene, it was treated as individual miRNA and ARBSs were search upstream from miRNA start site.

Total RNA extraction

TRI-reagent (Molecular Research Center Inc., Cincinnati, OH, USA) was used to extract total RNA from freshly frozen clinical samples and from cell lines. Briefly, tumors were cut into 10 20-μm-thick sections, which were then lysed in TRI-reagent. RNA was extracted according to the manufacturer's recommendations.

Microarrays and analysis

miRNA microarrays. Microarray analysis of miRNA expression was performed using human miRNA V2 microarrays (Agilent Technologies, Santa Clara, CA, USA), which contain probe sets for 723 human miRNAs from Sanger miRBase v.10.1. miRNA microarrays were performed according to the manufacturer's protocol. Briefly, total RNA was labeled using the miRNA Complete Labeling and Hyb Kit (Agilent Technologies) and hybridized to miRNA V2 microarrays. Microarrays were scanned using Agilent's DNA Microarray Scanner BA, and data were extracted using Agilent's Feature Extraction software (v.10.7.1.1) and analyzed using GeneSpring GX 10 (Agilent Technologies). Data were normalized using quantile normalization. miRNAs that were assigned a present call of at least 50% in any one of the four tested conditions were subjected to differential expression analysis. The Welch's *t*-test followed by correction by Benjamini and Hochberg with a corrected *P*-value cutoff of <0.05 and fold change cutoff of >1.5 were used to identify differentially expressed miRNAs. The array data have been submitted to ArrayExpress (accession number E-MTAB-408).

mRNA microarrays. LNCaP cells were transfected with pre-miR-32, pre-miR-148a or pre-miR-control and used for microarray analysis. Cells were lysed in TRI-reagent 3 days after transfection (Molecular Research Center Inc.). Total RNA was used for amplification and labeling using the Quick Amp Labeling Two-Color Kit (Agilent Technologies) and hybridized to Agilent's Whole Human Genome Oligo Microarray (44k). Microarrays were scanned using Agilent's DNA Microarray Scanner, and data were extracted using Agilent's Feature Extraction software (v.10.7.1.1). The data were then log transformed, and ratios of Cy5/Cy3 were calculated using GeneSpring GX 10 (Agilent Technologies). Microarrays were performed in duplicate, and the results were averaged. The array data have been submitted to ArrayExpress (accession number E-MEXP-2943).

qRT–PCR

miRNA expression analysis qRT–PCR analysis was performed using CFX96 qPCR equipment (Bio-Rad Laboratories, Hercules, CA, USA). The TaqMan microRNA Assay (Applied Biosystems, Foster City, CA, USA) was utilized according to the manufacturer's recommendations. Target gene expression was normalized to *RNU44* expression.

For mRNA expression analysis, first-strand complementary DNA (cDNA) from total RNA was synthesized with AMV reverse transcriptase (FinnZymes, Espoo, Finland) according to the manufacturer's instructions. The expression of *BTG2*, *PIK3IP1* and *TATA-box binding protein* (*TBP*) was analyzed using the Maxima SYBR Green qPCR master mix (Fermentas, Burlington, Canada) and CFX96 qPCR machinery (Bio-Rad Laboratories). The expression of each target gene was normalized to *TBP* expression. The primer sequences used in the analysis are given in Supplementary Table S6.

ChIP–qPCR

Previously described LNCaP-pcDNA3.1 and LNCaP-ARhi cells (Waltering *et al*., 2010) were hormone starved for 4 days and induced with 1 nM DHT or ethanol for 2 h. ChIP using antibody against AR (Karvonen *et al*., 1997; Thompson *et al*., 2006; Sahu *et al*., 2011; Urbanucci *et al*., 2011) or IgG (Santa Cruz Biotechnology Inc.) and qPCR was performed using Maxima SYBR Green qPCR master mix (Fermentas) and CFX96 qPCR equipment (Bio-Rad Laboratories). The enrichment relative to input chromatin was calculated according to the ΔC_t method, and the fold over ethanol (vehicle) treatment enrichment was calculated as described previously (Urbanucci *et al*., 2011). The sequences of the primers used in the analysis are in Supplementary Table S6.

Androgen stimulation of the cells

LNCaP cells were cultured in 5% charcoal-stripped serum (HyClone, Inc., South Logan, UT, USA) for 3 days followed by addition of 0, 1, 10 or 100 nM of DHT (Steraloids Inc., Newport, RI, USA). Total RNA was extracted after 6 h of DHT treatment. For pre-miRNA transfections, cells were transfected after 3 days in 10% stripped medium. A total of 15 nM DHT was added to the medium at the time of transfection.

The pre- and anti-miRNA transfections

miRNA precursors and inhibitors were purchased from Ambion (Applied Biosystems/Ambion, Austin, TX, USA). Cells were transfected using INTERFERin transfection

reagent (Polyplus-transfection, Illkirch, France) according to the manufacturer's protocol. Cells were reverse transfected with 10 nM pre-miRNA or anti-miR construct. miRNA expression levels were analyzed by qRT–PCR at 3 days after transfection.

Growth curves
LNCaP cells were reverse transfected with pre-miRNA constructs and seeded into 24-well plates. Growth curve measurements were initiated the day after transfection (marked as day 1). Resazurin reagent (R&D systems, Minneapolis, MN, USA) was used to assay cell growth, and luminometric detection was done with a fluorometer (Wallac 1420 Victor; Perkin-Elmer, Fremont, CA, USA). Each experiment was repeated at least twice with four replicates.

Cell cycle analysis
For cell cycle analysis, the cells were collected 3 days after pre-miRNA transfection and resuspended in 6.1 mM glucose, 137 mM NaCl, 5.4 mM KCl, 1.5 mM Na_2HPO_4, 0.9 mM KH_2PO_4 and 0.5 mM EDTA. The cells were then fixed in ethanol for 24 h, stained with propidium iodide (Sigma-Aldrich, St Louis, MO, USA) and analyzed by flow cytometry (Accuri C6, BD Accuri Cytometers, Ann Arbor, MI, USA). The proportion of cells in each phase of the cell cycle was determined by ModFitLT 3.2 software (Becton Dickinson, Mountain View, CA, USA). Cell cycle analysis was done with three replicates.

Caspase-3 staining
At 3 days after transfection, cells were trypsinized and placed onto objective slides, fixed in ice-cold methanol and acetone and stained with an anti-cleaved-caspase-3 antibody (dilution 1:1000, Cell Signaling Technology, Beverly, MA, USA). The staining was visualized using the PowerVision+ Poly-HRP IHC Detection Kit (ImmunoVision Technologies Corporation, Brisbane, CA, USA). Counterstaining was done with methyl green. Cleaved-caspase-3-positive cells were counted under a light microscope. Stainings were done in triplicates.

Western blotting
Cytoplasmic and nuclear proteins were isolated as described previously (Jalava *et al*., 2009). Briefly, proteins were separated by sodium dodecyl sulfate–polyacrylamide gel electrophoresis using 12% (BTG2), 10% (PIK3IP1) or 15% (BIM) polyacrylamide gels and transferred to polyvinylidene fluoride membranes (Immobilon-P, Millipore Corp., Billerica, MA, USA). The membranes were incubated overnight with antibodies against BTG2 (1:500 dilution, Sigma-Aldrich, Saint Louis, MO, USA), PIK3IP1 (1:200 dilution, H-14, Santa Cruz Biotechnology Inc.), actin (1:400 dilution, pan AB-5 clone ACTN05, Lab Vision Corp., Fremont, CA, USA) or BIM (1:500 dilution, Cell Signaling Technology). After washing and incubating with secondary antibodies (BTG2, PIK3IP1 and BIM: anti-rabbit IgG-horseradish peroxidase-conjugated antibody, Dako (Glostrup, Denmark); and Actin: anti-mouse IgG-horseradish peroxidase-conjugated antibody, Dako), protein bands were visualized by autoradiography.

Luciferase assays
pSGG-3UTR plasmids containing the 3′UTR of *BTG2* or *PIK3IP1* were purchased from Switchgear genomics (Menlo Park, CA, USA). LNCaP cells were co-transfected with pSGG-3UTR plasmid and pre-miRNA (pre-miR-control, pre-miR-32 or pre-miR-148a) using Dreamfect transfection reagent (Oz Biosciences, Marseille, France), according to the manufacturer's recommendations. Cells were lysed 24 h after transfection in reporter lysis buffer (Promega, Madison, WI, USA), and luciferase activity was analyzed using the Luciferase Assay System (Promega). For normalization, protein concentrations were measured from each cell lysate using the Bio-Rad LC protein assay (Bio-Rad). Luciferase assays were done in triplicate.

Cloning and co-transfections
The coding sequence of human BTG2 excluding 3′UTR was cloned to pSG5 expression vector from human cDNA clone SC115914 (OriGene, Rockville, MD, USA). Cells were transfected using Lipofectamine 2000 transfection reagent (Invitrogen, Carlsbad, CA, USA) according to the manufacturer's protocol. Briefly, cells were counted and seeded at 50 000 cells/well in 24-well plates and reverse transfected with 10 nM pre-miRNA construct and 150 ng of plasmid/well. Growth curve was assessed as described above.

Immunohistochemistry
Deparaffinized tissue microarray sections were pre-treated by autoclaving in 10 mM sodium citrate buffer (pH 6.0) at 121 °C for 2 min. The BTG2 and PIK3IP1 proteins were detected with rabbit polyclonal antibodies against BTG2 (Sigma-Aldrich, 1:1000 dilution) and PIK3IP1 (S-14, Santa Cruz Biotechnology 1:300 dilution), respectively, using PowerVision+ Poly-HRP IHC Detection Kit (Immunovision). The sections were counterstained with hematoxylin. Staining intensity was scored (0 = negative, 1 = weak, 2 = moderate and 3 = strong) by one of the authors (TV) in a blinded fashion.

Statistical analyses
Mann–Whitney *U*-tests, χ^2 tests, Welch's *t*-tests and ANOVAs with Bonferroni's test were used to determine statistical significance as described in the Results section. Kaplan–Meier survival curves with Mantel–Cox tests were employed to evaluate the prognostic value of the immunostainings.

Conflict of interest

The authors declare no conflict of interest.

Acknowledgements

We thank Ms Mariitta Vakkuri, Ms Päivi Martikainen and Mr Rolle Rahikainen for skillful technical assistance. The research leading to these results was funded by the European Community's Seventh Framework Programme (FP7/2007-2013) under grant agreement no. HEALTH-F2-2007-201438. In addition, grant support has been received from the Academy of Finland, the Cancer Society of Finland, the Reino Lahtikari Foundation, the Sigrid Juselius Foundation and the Medical Research Fund of Tampere University Hospital.

References

Ambs S, Prueitt RL, Yi M, Hudson RS, Howe TM, Petrocca F *et al*. (2008). Genomic profiling of microRNA and messenger RNA reveals deregulated microRNA expression in prostate cancer. *Cancer Res* **68**: 6162–6170.

Attard G, Reid AH, Yap TA, Raynaud F, Dowsett M, Settatree S *et al*. (2008). Phase I clinical trial of a selective inhibitor of CYP17, abiraterone acetate, confirms that castration-resistant prostate cancer commonly remains hormone driven. *J Clin Oncol* **26**: 4563–4571.

Bartel DP. (2009). MicroRNAs: target recognition and regulatory functions. *Cell* **136**: 215–233.

Cai C, Wang H, Xu Y, Chen S, Balk SP. (2009). Reactivation of androgen receptor-regulated TMPRSS2:ERG gene expression in castration-resistant prostate cancer. *Cancer Res* **69**: 6027–6032.

Chen CD, Welsbie DS, Tran C, Baek SH, Chen R, Vessella R *et al*. (2004). Molecular determinants of resistance to antiandrogen therapy. *Nat Med* **10**: 33–39.

Courtney KD, Corcoran RB, Engelman JA. (2010). The PI3K pathway as drug target in human cancer. *J Clin Oncol* **28**: 1075–1083.

Di Leva G, Croce CM. (2010). Roles of small RNAs in tumor formation. *Trends Mol Med* **16**: 257–267.

Edwards J, Krishna NS, Grigor KM, Bartlett JM. (2003). Androgen receptor gene amplification and protein expression in hormone refractory prostate cancer. *Br J Cancer* **89**: 552–526.

Feldman BJ, Feldman D. (2001). The development of androgen-independent prostate cancer. *Nat Rev Cancer* **1**: 34–45.

Ficazzola MA, Fraiman M, Gitlin J, Woo K, Melamed J, Rubin MA *et al*. (2001). Antiproliferative B cell translocation gene 2 protein is down-regulated post-transcriptionally as an early event in prostate carcinogenesis. *Carcinogenesis* **22**: 1271–1279.

Friedman RC, Farh KK, Burge CB, Bartel DP. (2009). Most mammalian mRNAs are conserved targets of microRNAs. *Genome Res* **19**: 92–105.

Fujita Y, Kojima K, Ohhashi R, Hamada N, Nozawa Y, Kitamoto A *et al*. (2010). MiR-148a attenuates paclitaxel resistance of hormone-refractory, drug-resistant prostate cancer PC3 cells by regulating MSK1 expression. *J Biol Chem* **285**: 19076–19084.

Guo H, Ingolia NT, Weissman JS, Bartel DP. (2010). Mammalian microRNAs predominantly act to decrease target mRNA levels. *Nature* **466**: 835–840.

Hong JW, Ryu MS, Lim IK. (2005). Phosphorylation of serine 147 of tis21/BTG2/pc3 by p-Erk1/2 induces Pin-1 binding in cytoplasm and cell death. *J Biol Chem* **280**: 21256–21263.

Hu XD, Meng QH, Xu JY, Jiao Y, Ge CM, Jacob A *et al*. (2011). BTG2 is an LXXLL-dependent co-repressor for androgen receptor transcriptional activity. *Biochem Biophys Res Commun* **404**: 903–909.

Jalava SE, Porkka KP, Rauhala HE, Isotalo J, Tammela TL, Visakorpi T. (2009). TCEB1 promotes invasion of prostate cancer cells. *Int J Cancer* **124**: 95–102.

Karvonen U, Kallio PJ, Jänne OA, Palvimo JJ. (1997). Interaction of androgen receptors with androgen response element in intact cells. *J Biol Chem* **272**: 15973–15979.

Kloosterman WP, Plasterk RH. (2006). The diverse functions of microRNAs in animal development and disease. *Dev Cell* **11**: 441–450.

Langmead B, Trapnell C, Pop M, Salzberg SL. (2009). Ultrafast and memory-efficient alignment of short DNA sequences to the human genome. *Genome Biol* **10**: R25.

Leinonen KA, Tolonen TT, Bracken H, Stenman UH, Tammela TL, Saramäki OR *et al*. (2010). Association of SPINK1 expression and TMPRSS2:ERG fusion with prognosis in endocrine-treated prostate cancer. *Clin Cancer Res* **16**: 2845–2851.

Linja MJ, Savinainen KJ, Saramäki OR, Tammela TL, Vessella RL, Visakorpi T. (2001). Amplification and overexpression of androgen receptor gene in hormone-refractory prostate cancer. *Cancer Res* **61**: 3550–3555.

Lu J, Getz G, Miska EA, Alvarez-Saavedra E, Lamb J, Peck D *et al*. (2005). MicroRNA expression profiles classify human cancers. *Nature* **435**: 834–838.

Martens-Uzunova ES, Jalava SE, Dits NF, van Leenders GJLH, Møller S, Trapman J *et al*. (2011). Diagnostic and prognostic signatures from the small non-coding RNA transcriptome in prostate cancer. *Oncogene* **31**: 978–991.

Massard C, Fizazi K. (2011). Targeting continued androgen receptor signaling in prostate cancer. *Clin Cancer Res* **17**: 3876–3883.

Möllerström E, Kovács A, Lövgren K, Nemes S, Delle U, Danielsson A *et al*. (2010). Up-regulation of cell cycle arrest protein BTG2 correlates with increased overall survival in breast cancer, as detected by immunohistochemistry using tissue microarray. *BMC Cancer* **10**: 296.

Murata T, Takayama K, Katayama S, Urano T, Horie-Inoue K, Ikeda K *et al*. (2010). miR-148a is an androgen-responsive microRNA that promotes LNCaP prostate cell growth by repressing its target CAND1 expression. *Prostate Cancer Prostatic Dis* **13**: 356–361.

Porkka KP, Pfeiffer MJ, Waltering KK, Vessella RL, Tammela TL, Visakorpi T. (2007). MicroRNA expression profiling in prostate cancer. *Cancer Res* **67**: 6130–6135.

Ribas J, Ni X, Haffner M, Wentzel EA, Salmasi AH, Chowdhury WH *et al*. (2009). miR-21: an androgen receptor-regulated microRNA that promotes hormone-dependent and hormone-independent prostate cancer growth. *Cancer Res* **69**: 7165–7169.

Sahu B, Laakso M, Ovaska K, Mirtti T, Lundin J, Rannikko A *et al*. (2011). Dual role of FoxA1 in androgen receptor binding to chromatin, androgen signalling and prostate cancer. *EMBO J* **30**: 3962–3976.

Sandberg R, Neilson JR, Sarma A, Sharp PA, Burge CB. (2008). Proliferating cells express mRNAs with shortened 3′ untranslated regions and fewer microRNA target sites. *Science* **320**: 1643–1647.

Saramäki OR, Harjula AE, Martikainen PM, Vessella RL, Tammela TL, Visakorpi T. (2008). TMPRSS2:ERG fusion identifies a subgroup of prostate cancers with a favorable prognosis. *Clin Cancer Res* **14**: 3395–3400.

Schaefer A, Jung M, Mollenkopf HJ, Wagner I, Stephan C, Jentzmik F *et al*. (2010). Diagnostic and prognostic implications of microRNA profiling in prostate carcinoma. *Int J Cancer* **126**: 1166–1176.

Scher HI, Sawyers CL. (2005). Biology of progressive, castration-resistant prostate cancer: directed therapies targeting the androgen-receptor signaling axis. *J Clin Oncol* **23**: 8253–8261.

Spahn M, Kneitz S, Scholz CJ, Stenger N, Rüdiger T, Ströbel P *et al*. (2010). Expression of microRNA-221 is progressively reduced in aggressive prostate cancer and metastasis and predicts clinical recurrence. *Int J Cancer* **127**: 394–403.

Stanbrough M, Bubley GJ, Ross K, Golub TR, Rubin MA, Penning TM *et al*. (2006). Increased expression of genes converting adrenal androgens to testosterone in androgen-independent prostate cancer. *Cancer Res* **66**: 2815–2825.

Sun T, Wang Q, Balk S, Brown M, Lee GS, Kantoff P. (2009). The role of microRNA-221 and microRNA-222 in androgen-independent prostate cancer cell lines. *Cancer Res* **69**: 3356–3363.

Taylor BS, Schultz N, Hieronymus H, Gopalan A, Xiao Y, Carver BS *et al*. (2010). Integrative genomic profiling of human prostate cancer. *Cancer Cell* **18**: 11–22.

Thompson J, Lepikhova T, Teixido-Travesa N, Whitehead MA, Palvimo JJ, Jänne OA. (2006). Small carboxyl-terminal domain phosphatase 2 attenuates androgen-dependent transcription. *EMBO J* **25**: 2757–2767.

Tomlins SA, Bjartell A, Chinnaiyan AM, Jenster G, Nam RK, Rubin MA *et al*. (2009). ETS gene fusions in prostate cancer: from discovery to daily clinical practice. *Eur Urol* **56**: 275–286.

Urbanucci A, Sahu B, Seppälä J, Larjo A, Latonen LM, Waltering KK *et al*. (2011). Overexpression of androgen receptor enhances the binding of the receptor to the chromatin. *Oncogene* **31**: 2153–2163.

Visakorpi T, Hyytinen E, Koivisto P, Tanner M, Keinänen R, Palmberg C *et al*. (1995). In vivo amplification of the androgen receptor gene and progression of human prostate cancer. *Nat Genet* **9**: 401–406.

Volinia S, Calin GA, Liu CG, Ambs S, Cimmino A, Petrocca F *et al*. (2006). A microRNA expression signature of human solid tumors

defines cancer gene targets. *Proc Natl Acad Sci USA* **103**: 2257–2261.

Waltering KK, Helenius MA, Sahu B, Manni V, Linja MJ, Jänne OA *et al*. (2009). Increased expression of androgen receptor sensitizes prostate cancer cells to low levels of androgens. *Cancer Res* **69**: 8141–8149.

Waltering KK, Porkka KP, Jalava SE, Urbanucci A, Kohonen PJ, Latonen LM *et al*. (2010). Androgen regulation of micro-RNAs in prostate cancer. *Prostate* **71**: 604–614.

Winkler GS. (2010). The mammalian anti-proliferative BTG/Tob protein family. *J Cell Physiol* **222**: 66–72.

Zhang Y, Liu T, Meyer CA, Eeckhoute J, Johnson DS, Bernstein BE *et al*. (2008). Model-based analysis of ChIP-Seq (MACS). *Genome Biol* **9**: R137.

Zhu Z, He X, Johnson C, Stoops J, Eaker AE, Stoffer DS *et al*. (2007). PI3K is negatively regulated by PIK3IP1, a novel p110 interacting protein. *Biochem Biophys Res Commun* **358**: 66–72.

Supplementary Information accompanies the paper on the Oncogene website (http://www.nature.com/onc)